UNIVERSITÀ DEGLI STUDI DI PADOVA

Dipartimento di Fisica e Astronomia

Corso di Laurea Triennale in Fisica

Tesi di Laurea

Inverse Beta Decay events selection in JUNO using Machine Learning algorithms

Relatore

prof. Alberto Garfagnini

Correlatori

dott. XXXXXX

dott. XXXXXX

Laureando

Candidate

Badge Number

Anno Accademico YYYY/YYYY

Discussion date

Abstract

The Jiangmen Underground Neutrino Observatory (JUNO) will be the largest liquid scintillator-based neutrino detectors in the World, for the next decade. Thanks to its large active mass (20 kt) and state of the art performances (3% effective energy resolution at 1 MeV), it will be able to perform important measurements in neutrino physics. The proposed thesis will study the application of different Machine Learning inspired algorithms for the discrimination of signal events (interactions of anti-neutrinos coming from the nearby nuclear power plants) from background events.

Contents

Chapter 1

Introduction

1.1 Neutrinos Oscillation

The Standard Model of elementary particle interactions provides an accurate description of strong, weak, and electromagnetic interactions, but it treats these interactions as distinct and unrelated. Within this framework, neutrinos are assumed to be massless, but this assumption has been called into question by physicists. Neutrino oscillations, which occur when neutrinos change from one flavor to another, are a potential indication of neutrino mass.
The term "neutrino oscillations" refers to this phenomena and it involve the conversion of a neutrino of a particular flavor to another as it propagates through space.

Each known flavor eigenstate, $(\nu_e, \nu_\mu, \nu_\tau)$, linked to three respective charged leptons (e, μ, τ) via the charged current interactions can be considered a complex combination of neutrino mass eigenstates as follow:

$$\begin{pmatrix} v_e \\ v_\mu \\ v_\tau \end{pmatrix} = U_{\text{PMNS}} \begin{pmatrix} v_1 \\ v_2 \\ v_3 \end{pmatrix}$$

in wich ν_i are the three mass eigensates, that have 3 masses m_i $(i = 1, 2, 3)$, which are non-degenerate, with $m_i \neq m_j$ for $i \neq j$.

The matrix U_{PMNS}, called Pontecorvo-Maki-Nakagawa-Sakata (PMNS) matrix, is composed of three rotation matrices, R_{23}, R_{13}, and R_{12}, each corresponding to a different mixing angle, θ_{23}, θ_{13}, and θ_{12}, respectively and a parameter δ_{CP} called the Dirac CP-violating phase. For this case, the Majorana CP phases are $etai (i = 1, 2)$, which are only physically possible if neutrinos are Majorana-type particles and do not participate in neutrino oscillations. Therefore, U can be expressed as:

$$U_{\text{PMNS}} =$$
$$= \begin{pmatrix} 1 & 0 & 0 \\ 0 & c_{23} & s_{23} \\ 0 & -s_{23} & c_{23} \end{pmatrix} \begin{pmatrix} c_{13} & 0 & s_{13}\mathrm{e}^{-\mathrm{i}\delta_{CP}} \\ 0 & 1 & 0 \\ -s_{13}\mathrm{e}^{\mathrm{i}\delta_{CP}} & 0 & c_{13} \end{pmatrix} \begin{pmatrix} c_{12} & s_{12} & 0 \\ -s_{12} & c_{12} & 0 \\ 0 & 0 & 1 \end{pmatrix} \begin{pmatrix} \mathrm{e}^{\mathrm{i}\eta_1} & 0 & 0 \\ 0 & \mathrm{e}^{\mathrm{i}\eta_2} & 0 \\ 0 & 0 & 1 \end{pmatrix}$$

The theoretical framework for neutrino oscillations involves the calculation of the oscillation probability as a function of the distance traveled by the neutrino, the neutrino mixing matrix, and the difference in squared masses between the three neutrino mass states, Δm^2_{ij}. Specifically,two nuclear power reactors 53 km away from the detector, which mostly produce anti-electron neutrinos $\bar{\nu}_e$ with energy below 10 MeV, are the principal sources of neutrinos for the JUNO experiment. So, it is necessary for the JUNO experiment to calculate the survival probability $P(\bar{\nu}_e \to \bar{\nu}_e)$ of electron antineutrinos.

$$P(\bar{\nu}_e \to \bar{\nu}_e) = 1 - \sin^2 2\theta_{12} c^4_{13} \sin^2\left(\frac{\Delta m^2_{21} L}{4\mathcal{E}}\right) - \sin^2 2\theta_{13}\left[c^2_{12}\sin^2\left(\frac{\Delta m^2_{31} L}{4\mathcal{E}}\right) + s^2_{12}\sin^2\left(\frac{\Delta m^2_{32} L}{4\mathcal{E}}\right)\right]$$

where $s_{ij} \equiv \sin\theta_{ij}, c_{ij} \equiv \cos\theta_{ij}, \mathcal{E}$ is the neutrino energy, L the travelled distance and $\Delta m^2_{ij} \equiv m^2_i - m^2_j$.
Past experiments have already given estimates for $\Delta m^2_{21}, |\Delta m^2_{31}|$ and the 3 mixing angles.

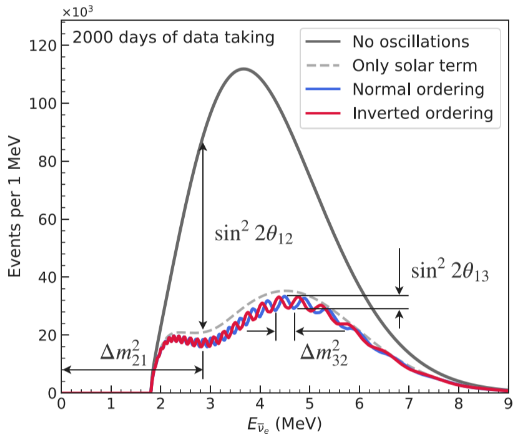

Figure 1.1: JUNO's reactor antineutrino energy spectrum is shown with and without the effect of neutrino oscillation. The gray dashed curve includes only the term in the disappearance probability modulated by $sin^2(2\theta_{12})$, while the blue and red curves use the full oscillation probability for normal and inverted mass orderings. Spectral features driven by oscillation parameters are illustrated, highlighting the rich information available in JUNO's high-resolution measurement of the oscillated spectrum.

The aim of JUNO is then to improve these results, and especially fix the sign of Δm^2_{31} by discriminating between two possibilities: *Normal Ordering* (**NO**), where $|\Delta m^2_{31}| = |\Delta m^2_{32}| + |\Delta m^2_{21}|$, and if $m_1 < m_2 < m_3$ we have the so called *Inverted Ordering* (**IO**), where $|\Delta m^2_{31}| = |\Delta m^2_{32}| - |\Delta m^2_{21}|$, and $m_3 < m_1 < m_2$. In fact, depending on the sign of Δm^2_{31}, the plot of 1.1 is minimally different.

1.2 The JUNO detector

The Jiangmen Underground Neutrino Observatory (JUNO) is an experiment that is currently under construction in Southern China, in Jinji town, 43 km to the southwest of Kaiping city. This multipurpose experiment is expected to detect a large number of antineutrinos from nuclear reactors, with most of them originating from the Taishan and Yangjiang nuclear power plants (NPPs). These two plants are located at a baseline of about 52.5 km from the JUNO detector, which was optimized for the best sensitivity to the neutrino mass ordering, and have a combined nominal thermal power of 26.6 GW_{th}. JUNO requires knowledge of the unoscillated reactor antineutrino spectrum shape, which is why a specialized small detector named TAO will be situated approximately 30 meters from one of the Taishan reactors to precisely measure it. The data collected by TAO will serve as a data-driven input to restrict the spectra of the other reactor cores.

The JUNO detector comprises three main components, namely the Central Detector (CD), a water Cherenkov detector, and a Top Tracker (TT). The CD is a liquid scintillator (LS) detector, featuring an effective energy resolution of $\sigma_E/E = 3\%/\sqrt{E(MeV)}$. It is composed of a 20 kton LS, enclosed within a spherical acrylic vessel, submerged in a water pool, that has a diameter of 43.5 m and a height of 44 m, providing sufficient buffer in all directions to protect the LS from the surrounding rock radioactivity. The water pool contains PMTs, which detect the Cherenkov light emitted from cosmic muons, acting as a veto detector. The vessel is supported by a stainless steel (SS) structure, via Connecting Bars, with CD Photomultiplier Tubes (PMTs) installed on the inner surface of the SS structure. Compensation coils are mounted on the SS structure, aimed at suppressing the Earth's magnetic field and reducing its impact on the photoelectron collection efficiency of the PMTs. Atop the water pool lies a Top Tracker, which comprises a plastic scintillator array designed to precisely measure muon tracks. The CD is connected to the outside through a chimney, which facilitates calibration operations. The Calibration House, located above the chimney, contains special radioactivity shielding and a muon detector.

A schematic illustrating the location of both JUNO and TAO is shown in Fig. 1.2.

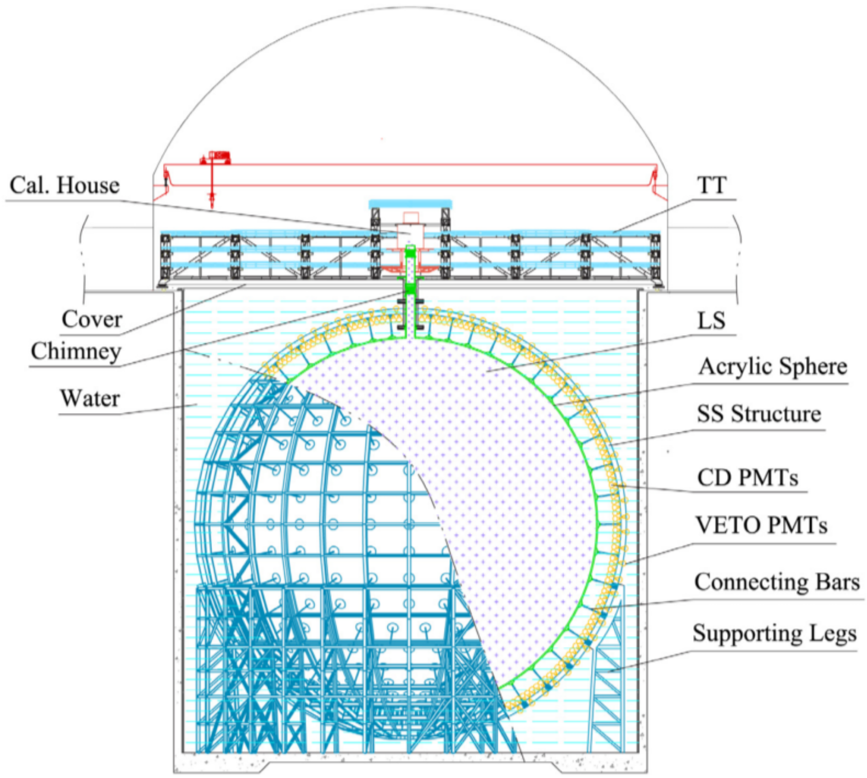

Figure 1.2: Schematic view of the JUNO experiment

1.3 JUNO signal and background

1.3.1 Signal

The scintillator is doped with a small amount of gadolinium to enhance its sensitivity to antineutrinos via the inverse beta decay (IBD) process. The liquid scintillator used in JUNO is a combination of LAB (linear alkyl benzene) and PPO (2,5-diphenyloxazole) doped with a small amount of bis-MSB (1,4-bis(2-methylstyryl) benzene). When a neutrino interacts with the scintillator, it can produce charged particles such as electrons, protons, and alpha particles that travel through the scintillator and excite the scintillation molecules. This excitation results in the emission of photons with a wavelength of around 430 nm. These photons are detected by 20,000 20-inch photomultiplier tubes (PMTs) distributed in a 3-dimensional arrangement inside the detector.

$$
\begin{aligned}
&\overline{\nu}e + p \rightarrow e^{+} + n \\
&n +^{A}_{Z} X \rightarrow^{A}_{Z-1} X^{*} + \gamma \\
&e^{+} + e^{-} \rightarrow 2\gamma
\end{aligned}
\tag{1.1}
$$

=

The PMTs detect the light and convert it into an electrical signal. The signals from all the PMTs are then combined to reconstruct the position and energy of the original neutrino interaction. This technique allows JUNO to measure the energy of the incoming neutrino to high precision, which is crucial for studying neutrino oscillation.

Moreover, the scintillator's composition and the detector's design are optimized to reduce background noise from other sources of radiation, such as cosmic rays and natural radioactivity. By carefully controlling these backgrounds, JUNO aims to achieve a signal-to-background ratio of better than 1:10,000, which is essential for observing the subtle effects of neutrino oscillation.

In JUNO's location, the energy spectrum will be distorted by two types of oscillations. The first is a slow (low frequency) oscillation driven by Δm^2_{21} and modulated by $\sin^2\theta_{12}$, while the second is a fast (high frequency) oscillation driven by Δm^2_{31} and modulated by $\sin^2\theta_{13}$. Fitting the data spectrum against the predicted spectrum distorted by standard neutrino oscillations enables measuring the oscillation parameters.

1.3.2 Background

Several different types of backgrounds signal are produced in the detector. For analysis we deeply analysed only the three most important contributes:

Radiogenic Backgrounds Radiogenic backgrounds arise from decays of radioactive isotopes in detector materials and surrounding rock. These decays can produce various forms of radiation, such as gamma rays and neutrons, which can interact with the detector and produce background events. Examples of radiogenic isotopes include ^{238}U, ^{232}Th, ^{40}K, and their daughter products. The main contributions to the radiogenic backgrounds come from the ^{238}U and ^{232}Th decay chains, with a smaller contribution from ^{40}K.

Cosmogenic Backgrounds Cosmogenic backgrounds arise from interactions of cosmic rays with materials surrounding the detector, such as the atmosphere and the Earth's crust. Muons produced in these interactions can penetrate the detector and produce background events. Specifically they interact with detector materials, producing isotopes such as ^{11}C, ^{9}Li, and ^{8}He, instable atoms which decay and produce additional background events.

Atmospheric Neutrino Backgrounds Atmospheric neutrino backgrounds arise from interactions of cosmic ray protons and nuclei with the Earth's atmosphere, which produce a flux of neutrinos that can interact with the detector. These interactions can produce both charged and neutral current events, which can mimic the signal from reactor neutrinos.

Reactor Antineutrino Backgrounds Reactor antineutrino backgrounds arise from the neutrinos produced in the nuclear reactors that power the JUNO experiment. These antineutrinos are the main signal for JUNO, but a small fraction of them can interact with the detector in ways that mimic background events. These interactions can produce both charged and neutral current events, which can be difficult to distinguish from the signal.

Here a viasualization sumary of all the bacgrounds contributions:

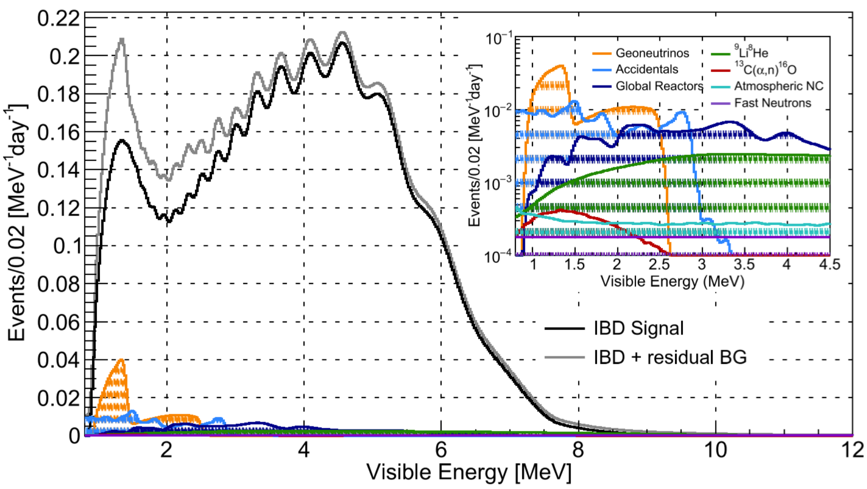

Figure 1.3: Visible energy spectrum as measured by the LPMT system with (grey) and without (black) backgrounds is that which is anticipated for JUNO. The energy resolution is one of the assumptions listed in the text. The predicted backgrounds, which make up around 7% of the whole sample of IBD candidates and are primarily confined below, are shown in the inset as spectra. ≈ 3 MeV

Chapter 2

Framework

2.1 Introduction to Machine Learning

Machine learning is a powerful tool that can be used to identify patterns in complex datasets. In the context of particle physics, machine learning algorithms can be used to detect signals from background noise in large datasets generated by detectors. In particular, for the detection of IBD signals from background, machine learning algorithms can be used to identify patterns in the data that are indicative of an IBD event, and to distinguish these signals from the background noise. Moreover, one advantage of machine learning for particle physics is that it can handle large amounts of data and identify subtle patterns that may be difficult for humans to detect.

There are several machine learning algorithms that can be used for this purpose, including decision trees, deep neural networks and support vector machines. These algorithms can be trained on simulated data to recognize IBD events signals over the background.

2.1.1 Supervised Learning

In supervised learning, the algorithm is trained on a labeled dataset, where the input data is accompanied by the correct output. The goal of the algorithm is to learn a function that can map input data to output data. Some examples of supervised learning algorithms include linear regression, logistic regression, decision trees, and support vector machines.

To understand the consepts of supervised learning it is useful to discuss a simle machin learning algorithm, linear regression.

2.2 Linear Regression

Linear regression is a type of supervised learning algorithm used in machine learning for predictive analysis. It is used to model the relationship between a dependent variable (also called the target variable) and one or more independent variables (also called the features or predictors).

The basic idea behind linear regression is to find the best-fitting line that describes the relationship between the independent and dependent variables. This line is often called the regression line or the line of best fit. The equation of this line can be written as:

$$y = \beta_0 + \beta_1 x_1 + \beta_2 x_2 + ... + \beta_p x_p + \epsilon \tag{2.1}$$

where y is the dependent variable, $x_1, x_2, ..., x_p$ are the independent variables, $\beta_0, \beta_1, \beta_2, ..., \beta_p$ are the coefficients or parameters of the model, and ϵ is the error term. The error term captures the deviation of the actual values of the dependent variable from the predicted values.

In order to determine the values of the coefficients $\beta_0, \beta_1, \beta_2, ..., \beta_p$, a common approach is to minimize a loss function, which measures the difference between the predicted values of the dependent variable and the actual values. The most commonly used loss function in linear regression is the mean squared error (MSE) function, which is defined as:

$$L(\beta_0, \beta_1, \beta_2, ..., \beta_p) = \frac{1}{n}\sum_{i=1}^{n}(y_i - \hat{y}_i)^2 \tag{2.2}$$

where n is the number of observations, y_i is the actual value of the dependent variable for the i-th observation, and $\hat{y}_i$ is the predicted value of the dependent variable for the i-th observation.

The goal of linear regression is to find the values of the coefficients $\beta_0, \beta_1, \beta_2, ..., \beta_p$ that minimize the loss function $L(\beta_0, \beta_1, \beta_2, ..., \beta_p)$. This can be achieved using various optimization techniques such as gradient descent or normal equations.

However, it is important to note that linear regression can suffer from overfitting or underfitting. Overfitting occurs when the model is too complex and captures noise in the data, while underfitting occurs when the model is too simple and fails to capture the underlying patterns in the data. To prevent overfitting or underfitting, regularization techniques such as Ridge regression or Lasso regression can be used.

References

[Kaj16] Takaaki Kajita. “Nobel Lecture: Discovery of atmospheric neutrino oscillations”. In: *Reviews of Modern Physics* 88.3 (July 2016). DOI: 10.1103/revmodphys.88.030501.